Shear strength and shear stiffness of CLT-beams loaded in plane

M. Flaig, H. J. Blaß
Holzbau und Baukonstruktionen
Karlsruhe Institute of Technology, Germany

1 General

Beams made of cross laminated timber (CLT) offer several advantages over solid or glued laminated timber beams due to their typical layup of orthogonally bonded layers. One major benefit of CLT is the high tensile strength perpendicular to the beam axis making CLT-beams less susceptible to cracks. Therefore, the use of CLT for the production of beams with tensile stresses perpendicular to the beam axis provides a considerably improved robustness.

In Europe, the requirements for the production and design of CLT-products are currently governed by technical approvals. However, a draft European standard specifying the performance requirements of cross laminated timber products has already been published in 2011. Although most of today's CLT-products are very similar in their structure and also efforts are made to develop standardised methods for design and verification of CLT, there is, so far, no general approach for the shear design of CLT-members loaded in plane. In fact, the strength properties and also the design methods given in different technical approvals for the verification of in plane shear stresses vary significantly and, moreover, for most products no information on the shear stiffness in plane direction is given at all. One main reason for the disparities seems to be the more complex calculation of shear stresses and deformations in CLT-members compared to traditional timber materials and therefore, in many cases, vastly simplified methods are used.

The intention of the present paper is to contribute to the development of standardised methods for the shear design of CLT-members loaded in plane. Therefore, at first, analytical solutions for the calculation of shear stresses and shear deformations in CLT-beams loaded in plane are presented. The equations are then validated by test results.

2 Shear strength of CLT-beams loaded in plane

2.1 Failure modes

In CLT-beams, like in solid materials, transversal forces acting in plane direction will cause shear stresses. The shear stress distribution can be assumed to be constant over the element thickness. In CLT-beams where adjacent lamellae within individual layers are not glued to each other at their edges, however, the thickness is not constant throughout the beam. In sections that coincide with unglued joints between neighboured lamellae shear forces can hence only be transferred by lamellae arranged perpendicular to the joints. The shear stresses in these net cross sections will consequently be greater than in the gross cross sections in-between unglued joints. The transfer of shear forces between longitudinal and transversal layers also causes shear stresses in the crossing areas of orthogonally bonded lamellae. Considering both shear stresses in the lamellae and the

crossing areas three different failure modes can be distinguished in CLT-beams subjected to shear stresses as shown in Figure 1.

Failure mode I is characterised by shear failure parallel to the grain in the gross cross section of a beam. The failure occurs in sections between unglued joints with equal shear stresses in longitudinal layers and transversal layers.

Failure mode II is characterised by shear failure perpendicular to the grain in the net cross section of a beam. The failure occurs in sections coinciding with unglued joints with shear stresses only in lamellae perpendicular to the joints.

Failure mode III is characterised by shear failure within the crossing-areas between orthogonally bonded lamellae. The failure is caused by torsional and unidirectional shear stresses resulting from the transfer of shear forces between adjacent layers.

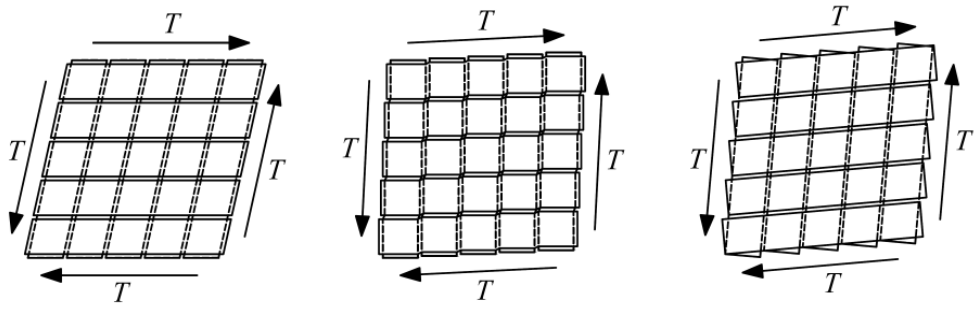

Figure 1: Failure modes I, II and III in CLT-beams subjected to transversal forces in plane direction (from left to right)

2.2 Calculation of shear stresses

For design and verification of CLT beams the shear stresses, corresponding to each of the three failure modes need to be calculated. In failure modes I and II shear stresses in the gross and the net cross section, respectively, need to be evaluated. In failure mode III three different components of shear stresses can be distinguished. The calculation of the five different shear stress components is described in the following sections.

2.2.1 Shear stresses in the lamellae

In CLT-beams the bonding between adjacent longitudinal lamellae, although connected only indirectly via transversal layers, is strong enough to ensure the layers to act as solid units. Shear stresses τ_{xz} in the lamellae causing failure parallel and perpendicular to the grain in failure modes I and II, respectively, can therefore be calculated according to Bernoulli-Euler Beam Theory by taking into account the appropriate thickness of the cross section considered.

$$\tau_{xz,gros} = \frac{V_z \cdot S_{y,gross}}{I_{y,gross} \cdot t_{gross}}$$ Shear stress in the gross cross section (Failure Mode I) Eq. 1

$$\tau_{xz,net} = \frac{V_z \cdot S_{y,net}}{I_{y,net} \cdot t_{net}}$$ Shear stress in the net cross section (Failure Mode I) Eq. 2

where t_{gross} is the total thickness of the element
and t_{net} is the smaller of the sum of the thickness of longitudinal or transversal layers

The parabolic functions in Eq. 1 and Eq. 2 describe curves that envelope the actual shear stresses in the net and the gross cross section. In CLT-beams normally the proportion of transversal layers will be kept as small as possible. Therefore, in most cases the net cross section of transversal

layers is decisive for the calculation of shear stresses $\tau_{xz,net}$. Starting from the upper and lower edge of a cross section, at first shear stresses both in longitudinal and transversal layers follow the parabolic function calculated with the gross cross section. In unglued joints between adjacent lamellae, however, shear stresses must be zero. In horizontal sections through unglued joints between longitudinal lamellae the shear stresses acting in transversal layers consequently can be found on a parabola calculated with the net cross section of transversal layers. As an example the distribution of shear stresses in the gross and the net cross section of a three layered CLT-beam is shown in Figure 2. The width of grooves and peaks in the curves of shear stresses depend on the stiffness of crossing areas and the stiffness ratios within a beam and is depicted only in a general manner in the graphs.

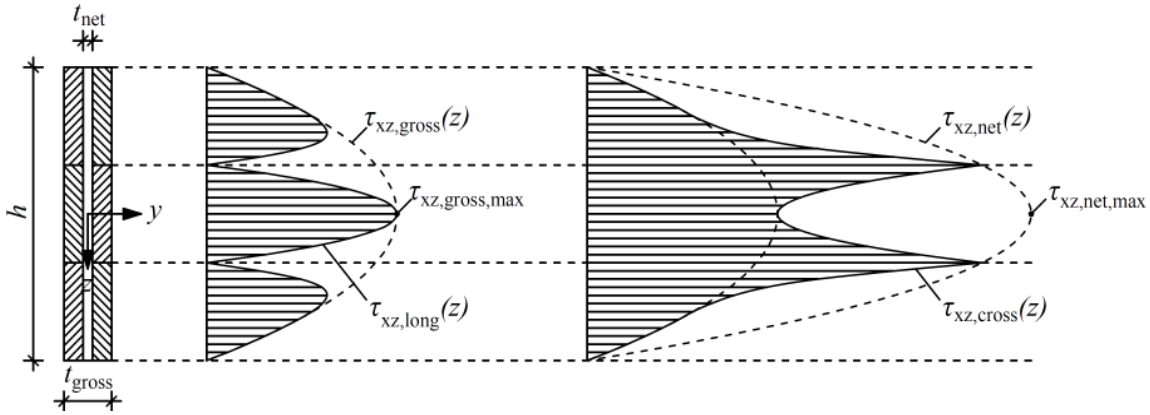

Figure 2: Distribution of shear stresses in the lamellae of a three-layered CLT-beam in cross sections within transversal lamellae: shear stresses $\tau_{xz,long}$ in longitudinal lamellae (left) and shear stresses $\tau_{xz,cross}$ in transversal lamella (right)

A conservative estimate of the actual maximum shear stress in longitudinal and transversal layers can be made by calculating the peak values of the parabolic functions according to Eq. 3 and Eq. 4.

$$\tau_{xz,gross,max} = \frac{3 \cdot V_z}{2 \cdot h \cdot t_{gross}} \qquad \text{Theoretical maximum shear stress in longitudinal layers} \qquad \text{Eq. 3}$$

$$\tau_{xz,net,max} = \frac{3 \cdot V_z}{2 \cdot h \cdot t_{net}} \qquad \text{Theoretical maximum shear stress in transversal layers} \qquad \text{Eq. 4}$$

For beams with an even number of lamellae in longitudinal layers Eq. 3 overestimates the maximum shear stress in the gross cross section whereas in beams with an odd number of lamellae in longitudinal layers too large shear stresses in the net cross section result from Eq. 4. For the cross section depicted in Figure 2 the difference between the theoretical and the actual maximum shear stress in the transversal layer amounts to 11%. However, the error decreases rapidly with an increasing number *m* of lamellae in longitudinal layers.

Table 1: Error in shear stresses calculated according to the expressions given in Eq. 3 and Eq. 4

number *m* of lamellae in longitudinal layers	2	3	4	5	6	7	8	9	10	11	12
error in the gross cross section in %	25	-	6.3	-	2.8	-	1.6	-	1.0	-	0.7
error in the net cross section in %	-	11	-	4.0	-	2.0	-	1.2	-	0.8	-

2.2.2 Shear stresses in the crossing areas

In failure mode III three different components of shear stresses occurring in the crossing areas have to be considered:

Shear stresses parallel to the beams axis which are caused by the change of the bending moment and the balancing of the resulting differential normal stresses in longitudinal lamellae,

Torsional shear stresses which arise due to the eccentricity between the centre lines of adjacent lamellae and

Shear stresses perpendicular to the beam axis occurring in the crossing areas at supports and concentrated load application points and in beams with variable cross section, such as notched beams, beams with holes and tapered beams.

The first two shear stress components can be derived from the model of a composite beam, where the longitudinal lamellae represent the individual parts of the beam. The third component corresponds to transverse tensile or compressive stresses occurring in glulam beams and can be calculated accordingly.

a) Shear stresses parallel to the beam axis

Since adjacent lamellae within longitudinal layers are not bonded at their edges differential normal forces dN_i caused by the change of the bending moment along the axis of a CLT-beam need to be transferred via the crossing areas between longitudinal and transversal layers. The normal forces N_i and the corresponding differentials dN_i acting in longitudinal lamellae can be calculated using the model of a composite beam shown in Figure 3. The resulting unidirectional shear stresses τ_{yx} in the crossing areas are obtained by dividing the differential normal force in a section of a longitudinal lamella through the crossing areas of the specific lamella within the considered section. As a result the distribution of shear stresses τ_{yx} within the element thickness depends on the ratio between the axial stiffness of longitudinal lamellae and the stiffness of the connections between longitudinal and transversal layers, i.e. the stiffness of crossing areas.

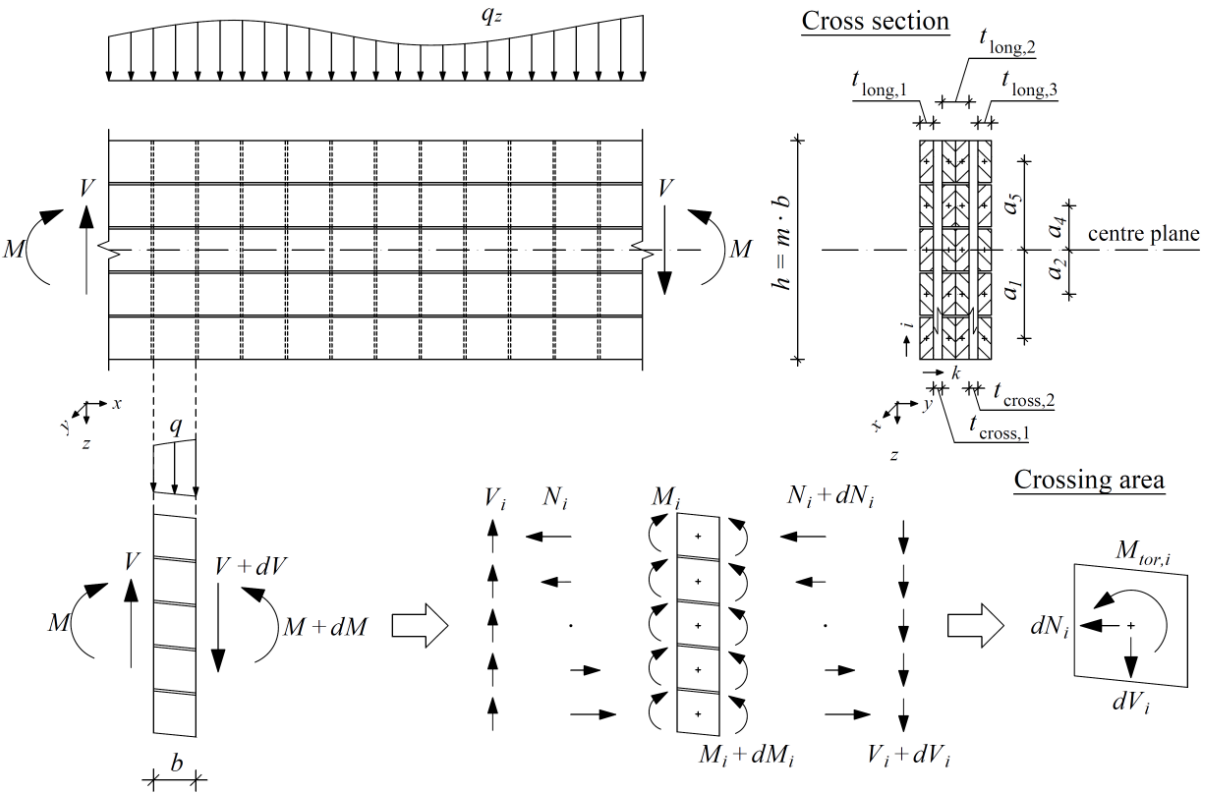

Figure 3: Side view and cross section of a four-layered CLT-beam loaded in plane (top) and internal forces in the beam, in individual lamellae and in the crossing areas (bottom, from left to right)

$$\tau_{yx} = \frac{dN_{i,max}}{n_{CA} \cdot b^2} \qquad \text{Eq. 5}$$

where $dN_{i,max} = \frac{dM}{I_{y,net,long}} \cdot a_{i,max} \cdot t_{net,long} \cdot b$ with $dM = V \cdot dx = V \cdot b$

$$I_{y,net,long} = \frac{m^3 \cdot b^3 \cdot t_{net,long}}{12} \quad \text{and} \quad a_{i,max} = \frac{m-1}{2} \cdot b$$

Substituting the given expressions for dN_i, $I_{net,long}$ and $a_{i,max}$ into Eq. 5 yields

$$\tau_{yx} = \frac{6 \cdot V}{b^2 \cdot n_{CA}} \cdot \left(\frac{1}{m^2} - \frac{1}{m^3} \right) \qquad \text{Eq. 6}$$

As can be seen, shear stresses τ_{yx} are linearly dependent on the reciprocal values of the squared width of lamellae b and the number of crossing areas n_{CA} within the element thickness. The last term in brackets describes the influence of the number of lamellae m within longitudinal layers. Eq. 5 and Eq. 6 provide accurate results for CLT-beams with a constant ratio of $t_{long,k}/n_{CA,k}$ between the thickness of an individual longitudinal layer and the number of glue lines the respective layer shares with adjacent transversal layers. In such beams shear stresses τ_{yx} in the crossing areas are constant within the element thickness since the ratio between the axial stiffness and the stiffness of adjacent crossing areas is equal for all longitudinal lamellae. In contrast to this, shear stresses τ_{yx} vary within the thickness of CLT-beams where the ratio of $t_{long,k}/n_{CA,k}$ is not equal for all longitudinal layers. However, within the range of layups that are used in practice the variation of shear stresses τ_{yx} within the element thickness is small, especially in CLT-beams made of softwood, with a modulus of elasticity of lamellae of about 11,000 N/mm² and a slip modulus of crossing areas of about 5 N/mm³ (see 3.2). Therefore Eq. 5 and Eq. 6 provide good approximations for the shear stresses τ_{yx} in such beams.

b) Torsional shear stresses

Due to the eccentricity of the normal forces N_i acting in the centre lines of adjacent longitudinal lamellae the differential normal forces dN_i transferred via the crossing areas not only induce shear stresses parallel to the beam axis, but also torsional shear stresses within the crossing areas. Like shear stresses τ_{yx} acting in the direction of the beam axis, torsional shear stresses τ_{tor} can be derived from the model of a composite beam shown in Figure 3. Assuming that torsional shear stresses are, like shear stresses τ_{yx}, constant within the beam thickness and in addition also uniformly distributed within the beam height, which is given on the condition that the lamellae in transversal layers stay straight in the deformed beam, torsional shear stresses in the crossing areas can be calculated according to Eq. 7. In Eq. 7 τ_{tor} is the stress vector acting parallel to the shorter edges of a crossing area causing rolling shear stresses in the narrower of the two bonded lamellae and b is the width of the broader lamellae.

$$\tau_{tor} = \frac{\sum_{i=1}^{m} M_{tor,i}}{n_{CA} \cdot \sum_{i=1}^{m} I_{p,CA}} \cdot \frac{b}{2} \qquad \text{Eq. 7}$$

where $\sum_{i=1}^{m} M_{tor,i} = \sum_{i=1}^{m} dN_i(x) \cdot a_i = \frac{dM(x)}{I_{y,net,long}} \cdot t_{net,long} \cdot b \cdot \sum_{i=1}^{m} a_i^2$,

$$\sum_{i=1}^{m} a_i^2 = b^2 \cdot \sum_{i=1}^{m} \left(\frac{m+1}{2} - i \right)^2 = b^2 \cdot \frac{(m^3 - m)}{12} \quad \text{and} \quad \sum_{i=1}^{m} I_{p,CA} = m \cdot \frac{b^4}{6}$$

The assumption of a constant width b of lamellae in all longitudinal and transversal layers and the substitution of the expressions above into Eq. 7 yields the closed-form solution given in Eq. 8. A closed-form solution for beams with lamellae of different widths in longitudinal and transversal layers can be found in Blaß and Flaig (2012).

$$\tau_{\text{tor}} = \frac{3 \cdot V}{b^2 \cdot n_{\text{CA}}} \cdot \left(\frac{1}{m} - \frac{1}{m^3} \right). \qquad \text{Eq. 8}$$

The torsional shear stresses τ_{tor} are, like shear stresses τ_{yx}, linearly dependent on the reciprocal values of the squared width of lamellae b and the number of crossing areas n_{CA} within the element thickness. The term in brackets describes again the influence of the number of lamellae m within longitudinal layers. In beams with a large number m of lamellae within longitudinal layers the third order term $1/m^3$ becomes very small and therefore may be neglected. This simplifies Eq. 8 to

$$\tau_{\text{tor}} = \frac{3 \cdot V}{b^2 \cdot n_{\text{CA}} \cdot m} = \frac{V \cdot b}{\Sigma I_{\text{p,CA}}} \cdot \frac{b}{2}. \qquad \text{Eq. 9}$$

The expression on the right side can also be found in many technical approvals, where it is given for the calculation of torsional shear stresses in shear walls and diaphragms.

c) Shear stress components perpendicular to the beam axis

Shear stresses τ_{yz} in the crossing areas of CLT-beams may result from both external forces, e.g. support reactions and loads, and internal forces arising from changes in the cross section or the direction of the beam axis. Equations for the calculation of shear stress components τ_{yz} in the crossing areas of CLT-beams with holes and notches as well as for tapered CLT-beams and CLT-beams with dowel type connections loaded perpendicular to the beam axis are specified in Blaß and Flaig (2012).

For beams subjected to external forces acting in plane and on the surface, shear stresses τ_{yz} can be calculated according to Eq. 10, provided that the loads are transferred by contact via the end grain surfaces of transversal layers only and on the assumption that shear stresses τ_{yz} are uniformly distributed within the beam height.

$$\tau_{\text{yz}} = \frac{q_z}{m \cdot b} \qquad \text{Eq. 10}$$

2.3 Strength properties and verification of shear stresses

In the design of CLT-beams each of the above-described shear stresses must be verified with the corresponding shear strengths related to the relevant shear failure mode. In the crossing areas also the interaction of simultaneously acting shear stress components has to be taken into consideration.

2.3.1 Failure Mode I

Since failure mode I is characterised by shear failure parallel to the grain within the lamellae, the shear strength specified in EN 338 is used for the verification of shear stresses. Since, in general, the cross sections of the individual lamellae are rather small and moreover the development of large, individual cracks is impeded by transversal layers, the influence of cracks on the shear strength of the lamellae is low. Therefore, a factor k_{cr} = 1,0 can be assumed, which is also specified in Germany's National Annex to Eurocode 5.

2.3.2 *Failure Mode II*

In failure mode II shear failure occurs in the net cross section within the joints between non edge bonded lamellae. Jöbstl et al. (2008) determined a mean value of the corresponding shear strength $f_{v,lam,90}$ perpendicular to the grain of 12.8 N/mm² and a characteristic value of 10.3 N/mm² by tests with single boards subjected to shear forces perpendicular to the grain. Considerably higher shear stresses perpendicular to the grain were evaluated from tests with beams with holes (Blaß and Flaig, 2012), however, none of the tested beams failed within the net cross section.

2.3.3 *Failure Mode III*

In CLT-beams subjected to transversal forces in plane direction failure in the crossing areas is caused by the interaction of at least two shear stress components, since both torsional shear stresses and shear stresses in direction of the beam axis always occur simultaneously. In addition shear stresses perpendicular to the beam axis may arise from external or internal forces. In the verification of shear stresses in failure mode III the interaction of the different shear stress components has to be considered.

In recent years the shear strength of crossing areas against both shear forces and torsional moments, has been determined in several test series. An overview of the shear strengths evaluated from tests with small specimens comprising one or two crossing areas is given in Table 2, lines 2 - 5.

Table 2: Torsional shear strength and rolling shear strength of crossing areas determined by tests with small specimens and with CLT-beams

Author	description of test setup	n	$f_{v,tor,mean}$ in N/mm²	$f_{v,tor,k}$ in N/mm²	$f_{R,mean}$ in N/mm²	$f_{R,k}$ in N/mm²
Blaß/Görlacher (2002)	single crossing areas	57	3.59	2.82	-	-
Jöbstl (2004)	single crossing areas	81	3.46	2.71	-	-
Wallner (2004)	two symmetric crossing areas	122	-	-	1.51	1.18
Blaß/Flaig (Figure 4)	two symmetric crossing areas	6	-	-	1.43	1.18
Blaß/Flaig (2012)	notched beams (bending tests)	13	3,98	2,76	1,71	1.19
Blaß/Flaig (2012)	beams with holes (bending tests)	13	3,69	2.79	1.58	1.20
Blaß/Flaig (2010)	CUAP (see Table 3)	12	4.67	2,68	1.99	1.15

From the different test series that were performed with small specimens it can be concluded that the shear strength of crossing areas against unidirectional shear stresses is equal to the rolling shear strength of timber. The torsional shear strength in contrast exceeds this value considerably, although the failure is also governed by rolling shear stresses. The torsional shear strengths found by Blaß and Görlacher and Jöbstl et al., respectively, are very similar, both mean and characteristic values, although the size of the tested crossing areas varied considerably (Blaß/Görlacher 40 x 40 mm, 40 x 64 mm, 62 x 95 mm, 62 x 75 mm, 64 x 64 mm, 64 x 100 mm; Jöbstl et al. 100 x 145 mm, 150 x 145 mm, 200 x 145 mm). The results within either test series also showed no significant influence of the crossing area size on the shear strength. The same applies to the shear strength against unidirectional shear stresses where the tested crossing areas had dimensions of 100 x 150 mm, 150 x 150 mm, 200 x 150 mm (Wallner) and 75 x 150 mm (Blaß/Flaig, Figure 4). Both rolling shear strength and torsional shear strength of crossing areas seem therefore to be size independent within the sizes tested and occurring in practice.

To identify a suitable criterion for the verification of shear stresses in the crossing areas – considering the interaction of unidirectional and torsional shear stress components – the results of bending tests where failure occurred due to shear stresses in the crossing areas were evaluated using equations Eq. 6, Eq. 8 and Eq. 10. The considered tests were performed with prismatic beams (see Table 3), notched beams and beams with holes (Blaß and Flaig, 2012).Tests with prismatic beams were performed according to CUAP 03.04/06 involving a kerf that was sawn into the longitudinal layers in the middle of the beam height. The tested CLT-beams with notches and holes were three- and six-layered with heights of 300 mm and 600 mm. The span of all tested beams was within the range of 7.5 to 10 times the beam height.

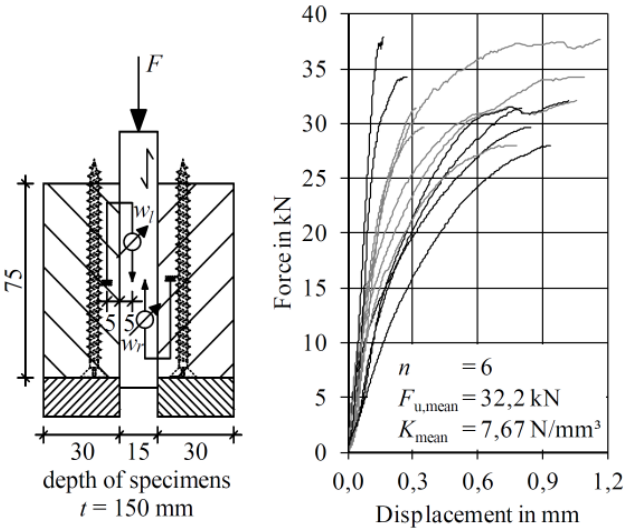

Figure 4: Compressive shear tests to determine the shear strength and the slip modulus of crossing areas subjected to unidirectional shear stresses

Table 3: Torsional shear strength and rolling shear strength of crossing areas evaluated from bending tests according to CUAP 03.04/06

75 / 75 / 27 27 27	series 27-27-27					
$f_{v,tor}$ in N/mm²	3.68	4.43	3.72	3.72	3.51	3.61
f_R in N/mm²	1.58	1.90	1.59	1.59	1.50	1.55
75 / 75 / 30 20 30	series 30-20-30					
$f_{v,tor}$ in N/mm²	4.64	6.49	6.05	3.66	6.26	6.33
f_R in N/mm²	1.99	2.78	2.59	1.57	2.68	2.71

To evaluate the strength properties of crossing areas from beam tests a total of six different failure criterions were investigated (Flaig, 2013). The best agreement between the shear properties evaluated from beam tests and the respective values obtained from tests with small specimens was found for the failure criterion given in Eq. 11, which takes into account the interaction of torsional and unidirectional shear stresses, but no interaction of unidirectional shear stresses in direction of and perpendicular to the beam axis.

$$\frac{\tau_{tor,d}}{f_{v,tor,d}} + \frac{\tau_{yx,d}}{f_{R,d}} \le 1 \qquad \text{and} \qquad \frac{\tau_{tor,d}}{f_{v,tor,d}} + \frac{\tau_{yz,d}}{f_{R,d}} \le 1 \qquad \text{Eq. 11}$$

To evaluate both strength properties, a constant ratio between torsional and rolling shear strength of 2.33 was assumed that was derived from the results of tests performed with small specimens given in Table 2. In beams with holes and notches also stress peaks near holes and notches were considered (Blaß and Flaig, 2012). In Table 2, lines 6, 7 and 8 the rolling shear strength and the torsional shear strength evaluated from test series with CLT-beams are given.

2.3.4 Effective shear strength of prismatic CLT-beams

Depending on the width of lamellae and on the thickness and the arrangement of longitudinal and transversal layers within the beam the shear resistance of a CLT-beam is governed by either of the three failure modes. The effective shear strength $f_{v,CLT}$ related to the gross cross section of CLT-beams can be calculated as the minimum value resulting from the three expressions given in Eq. 12, each representing one of the three failure modes.

$$f_{v,CLT} = \min \begin{cases} f_{v,lam} \\ f_{v,lam,90} \cdot \dfrac{t_{net}}{t_{gross}} \\ \dfrac{b \cdot n_{CA}}{2 \cdot t_{gross}} \cdot \dfrac{1}{\dfrac{1}{f_{v,tor}} \cdot \left(1 - \dfrac{1}{m^2}\right) + \dfrac{2}{f_R} \cdot \left(\dfrac{1}{m} - \dfrac{1}{m^2}\right)} \end{cases} \qquad \text{Eq. 12}$$

In Figure 5 characteristic shear strengths of CLT-beams determined from Eq. 12 are given in graphical form.

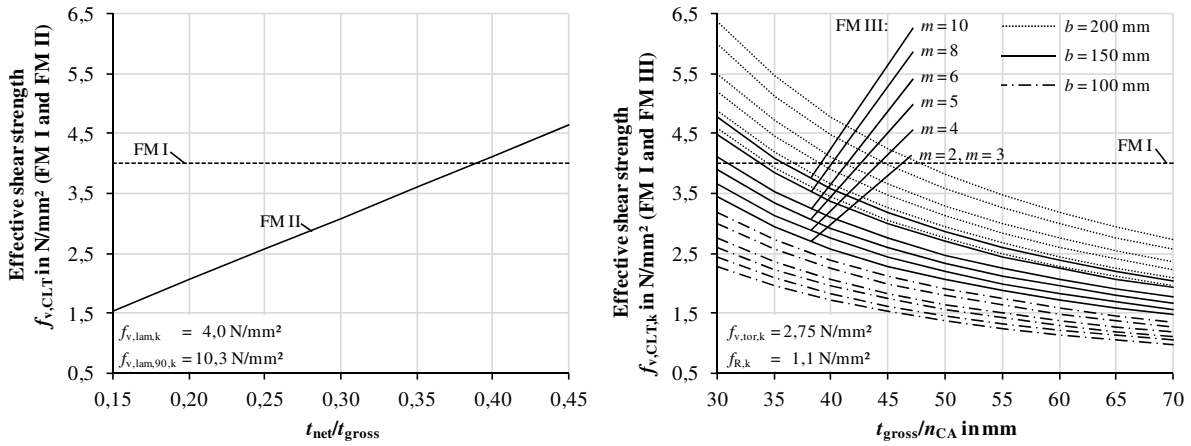

Figure 5: Effective shear strength $f_{v,CLT}$ of CLT-beams resulting from failure modes I and II (left) and failure modes I and III (right)

In the diagram on the left side the shear strength calculated from the second expression in Eq. 12, corresponding to failure mode II (FM II), is plotted against the ratio t_{net}/t_{gross}, which in CLT-beams normally equals the proportion of transversal layers. The shear strength calculated from the third expression in Eq. 12, representing failure mode III (FM III), is plotted in the diagram on the right side. Here, the beam layup is given on the abscissa in form of the ratio t_{gross}/n_{CA}, where t_{gross} is the total thickness of the beam and n_{CA} is the number of glue lines between longitudinal and transversal layers within the total thickness. The three different sets of curves demonstrate the influence of the width b of lamellae in failure mode III whereas the influence of the number m of lamellae within longitudinal layers is represented by the curves within each set.

The graphs were calculated assuming a characteristic value of the shear strength perpendicular to the grain of 10.3 N/mm² and characteristic torsional and rolling shear strength of 2.75 N/mm² and 1.1 N/mm², respectively. In both diagrams the effective shear strength resulting from failure mode I (FM I) is given, too. The characteristic value was determined with the shear strength of strength class C24 given in EN 338 and a crack reduction factor of 1.0.

3 Shear stiffness of CLT-beams loaded in plane

3.1 Analytical approach

In CLT-beams subjected to in plane transversal forces, shear stresses acting within the crossing areas will entail mutual displacements between the bonded lamellae. Therefore, the shear deformation of CLT-beams originates not only from shear strain within the lamellae but also from rotational and translational displacements in the crossing areas. Using the definitions given in Figure 6 the shear strain components γ_{yx} and γ_{tor} resulting from the displacements within the crossing areas can be calculated according Eq. 13 and Eq. 14, where K is the slip modulus of the crossing areas in N/mm³.

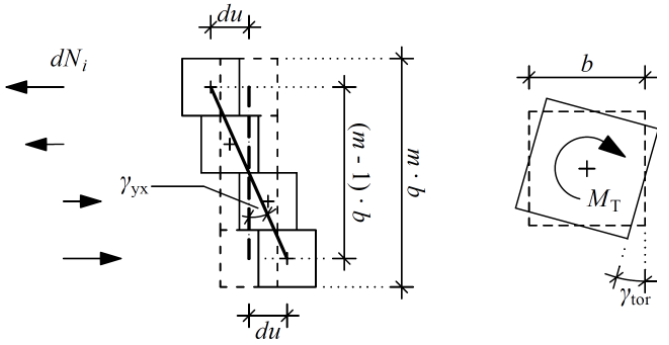

Figure 6: Shear strain components γ_{tor} and γ_{yx} resulting from shear stresses in the crossing areas of CLT-beams

$$\gamma_{yx} = \frac{2 \cdot du}{b \cdot (m-1)} = \frac{2 \cdot t_{yx}}{K \cdot b \cdot (m-1)} \qquad \text{Eq. 13}$$

$$\gamma_{tor} = \frac{2 \cdot t_{tor}}{K \cdot b} \qquad \text{Eq. 14}$$

By substituting the shear stresses τ_{yx} and τ_{tor} given in Eq. 6 and Eq. 8 into the expressions given in Eq. 13 and Eq. 14, respectively, the relations given in Eq. 15 and Eq. 16 are obtained.

$$\gamma_{tor} = \frac{6 \cdot V}{b^3 \cdot K} \cdot \left(\frac{1}{m} - \frac{1}{m^3} \right) \cdot \frac{1}{n_{CA}} \qquad \text{Eq. 15}$$

$$\gamma_{yx} = \frac{12 \cdot V}{b^3 \cdot K \cdot} \cdot \frac{1}{m^3} \cdot \frac{1}{n_{CA}} \qquad \text{Eq. 16}$$

Using the constitutive equation $\tau = \gamma \cdot G$ an effective shear modulus $G_{eff,CA}$ representing the shear deformation in the crossing areas can be calculated. For CLT-beams with rectangular cross section the shear modulus $G_{eff,CA}$ related to the gross cross section can be obtained from the expression given in Eq. 17.

$$G_{eff,CA} = \frac{6 \cdot V}{5 \cdot A_{gross} \cdot \left(\gamma_{tor} + \gamma_{yx} \right)} = \frac{K \cdot b^2}{5} \cdot \frac{n_{CA}}{t_{gross}} \cdot \frac{m^2}{\left(m^2 + 1 \right)} \qquad \text{Eq. 17}$$

The superposition of shear deformations in the lamellae and in the crossing areas yields the effective shear modulus $G_{eff,CLT}$ of CLT-beams given in Eq. 18, which again is related to the gross cross section.

$$G_{eff,CLT} = \left(\frac{1}{G_{lam}} + \frac{1}{G_{eff,CA}} \right)^{-1} \qquad \text{Eq. 18}$$

In Figure 7 the effective shear modulus of CLT-beams calculated from Eq. 18 is given as a function of the ratio t_{gross}/n_{CA} between the element thickness and the number of glue lines within the

element thickness and for different widths b and numbers m of lamellae in longitudinal layers The graphs plotted in the diagram apply to a shear modulus of the lamellae of 690 N/mm² and a slip modulus of the crossing areas of 5 N/mm³. The large distances between the sets of curves demonstrate the influence of the size of crossing areas – expressed through the width of lamellae b – on the shear stiffness of CLT-beams. The ratio of t_{gross}/n_{CA} also significantly affects the shear stiffness, whereas the number of lamellae within longitudinal layers has rather small influence, especially if m is greater than 2.

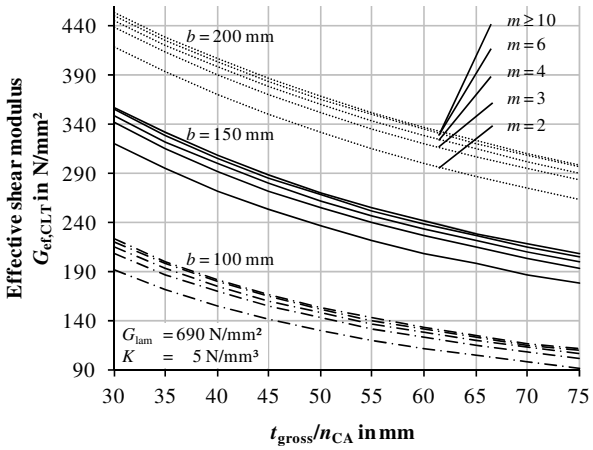

Figure 7: Effective shear modulus of CLT-beams

3.2 Test results

Until today only few test have been performed to determine the shear stiffness of CLT loaded in plane (Bosl, 2002; Traetta et al., 2006) but various tests have been performed to determine the stiffness of crossing areas of orthogonally bonded boards, both with torsional and unidirectional shear stresses. In Table 4 the results from tests with small specimens comprising one or two crossing areas are given. Tests to determine the torsional slip modulus of crossing areas have been performed by Blaß and Görlacher (2002) and by Jöbstl et al. (2004). The obtained values differ quite significantly but the disparity most likely originates from shear deformations within the bonded boards, which are, at least partly, included in the results presented by Jöbstl et al. but not contained in the values given by Blaß and Görlacher. However, the values presented by Blaß and Görlacher still include deformations due to compressive stresses perpendicular to the grain since the torsional moment was transferred to the specimens through contact by means of a clamping. From tests with crossing areas subjected to shear forces similar slip moduli have been determined by (Wallner 2004). However, these test results again comprise parts of the shear deformation within the boards. Considering the influence of the different test setups used to determine the slip moduli of crossing areas the disparity between the obtained values becomes much less pronounced.

Table 4: Slip modulus K of orthogonally bonded lamellae determined by tests performed with specimens with one or two crossing areas

Author	description of test setup	shear stress in crossing area	n	K_{mean} in N/mm³
Blaß/Görlacher (2002)	single crossing areas	torsion	30	4.87
Jöbstl (2004)	single crossing areas	torsion	81	3.45
Wallner (2004)	two symmetric crossing areas	unidirectional	122	4.26

From the difference between local and global modulus of elasticity of CLT-beams, measured in four-point bending tests, a distinctly higher slip modulus with an average of 7.58 N/mm³ was evaluated (Blaß and Flaig, 2012). The results of the performed tests are summarised in Table 5. The effective shear moduli and the slip moduli of crossing areas given in the table have been evaluated using Eq. 17 and Eq. 18, assuming a constant shear modulus of the lamellae of 690 N/mm².

The slip moduli evaluated from the bending tests are distinctly higher than the values obtained from tests with single crossing area whereas the agreement with the value of 7.67 N/mm² evaluated from the tests described in Figure 4 is very good.

Table 5: Local and global modulus of elasticity and effective shear modulus of CLT-beams and slip modulus of crossing areas evaluated from four-point-bending tests with CLT-beams

series 2-2	$E_{lok,gross}$	$E_{glob,gross}$ in N/mm²	$G_{eff,CLT}$	K in N/mm³	series 3-2	$E_{lok,gross}$	$E_{glob,gross}$ in N/mm²	$G_{eff,CLT}$	K in N/mm³
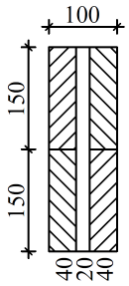	12160	10880	300	7.35	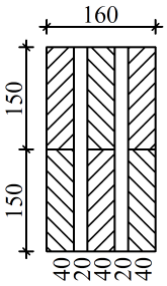	9255	8685	409	11.1
	13024	11528	291	6.99		9240	8558	336	7.27
	13752	11744	233	4.89		10568	9495	271	4.96
	10400	9376	276	6.39		9165	8573	384	9.64
	10952	9416	195	3.76		9983	9353	430	12.6
	7680	7216	346	9.64		7433	6893	275	5.08
	8120	7424	251	5.47		7613	7163	351	7.95
	7872	7016	187	3.56		6983	6630	381	9.43
	8048	7560	361	10.5		7200	6863	424	12.2
	8184	7448	240	5.11		6975	6930	-	-
mean			268	6.36				362	8.92

4 Summary and conclusions

In shear design of CLT-beams three different failure modes are distinguished considering shear stresses acting parallel and perpendicular to the grain within the lamellae and shear stresses within the crossing areas of orthogonally bonded lamellae, respectively. For the calculation of shear stresses occurring in the lamellae and the crossing areas of CLT-beams subjected to transversal loads acting in plane direction an analytical approach is presented. On the basis of experimental data, published by other researchers and obtained by own tests, strength properties and criteria for the verification of shear stresses corresponding to the different failure modes were specified. From the equations for the calculation of shear stresses and the respective failure criteria an expression for the calculation of the effective shear strength related to the gross cross section of CLT-beams was derived to simplify the verification of shear stresses and it was shown that the effective shear strength of CLT-beams is strongly dependent on cross sectional arrangement and thickness ratio of longitudinal and transversal layers and on the width of lamellae. The equations for the calculation of shear stresses were also used to derive solutions for the calculation of shear strain components resulting from mutual displacements in the crossing areas of CLT-beams. By the superposition of strain components resulting from shear stresses in the crossing areas and in the lamellae a closed-form expression for the calculation of an effective shear modulus of CLT-beams was obtained. The expression shows that the effective shear stiffness of CLT-beams, like the effective shear strength, strongly depends on the width of lamellae and their cross sectional arrangement. The presented analytical approach was used to evaluate strength and stiffness properties of crossing areas from tests performed with different types of CLT-beams comprising prismatic beams, notched beams and beams with holes. The obtained values were compared to strength and stiffness properties determined by tests with small specimens and good agreement was found.

Due to its simplicity and the good agreement with experimental results the presented approach represents a suitable and effective tool for the shear design of CLT-beams including both the calculation of shear stresses and shear deformations and it provides conservative results if strength and stiffness properties determined by tests with small specimens are used.

5 Symbols

a_i distance between the centre line of an individual longitudinal lamella and the xy-centre plane of the gross cross section

$a_{i,max}$ distance between the centre line of the uppermost/lowermost longitudinal lamella and the xy-centre plane of the gross cross section

b width of lamellae (here constant within all layers)

$dN_{i,k}$ differential normal force within an individual longitudinal lamella i,k

dM differential bending moment within the gross cross section

$f_{v,lam}$ shear strength of the lamellae according to EN 338

$f_{v,90,lam}$ shear strength perpendicular to the grain in joints between non edge bonded lamellae

$f_{v,tor}$ torsional shear strength of crossing areas of orthogonally bonded lamellae

f_R rolling shear strength

G_{CA} shear modulus of a CLT-beam resulting from the joint slip in crossing areas

$G_{eff,CLT}$ effective shear modulus of a CLT-beam

G_{lam} shear modulus of lamellae

h beam height

$I_{y,net,long}$ second moment of area of longitudinal layers about y-axis

$I_{p,CA}$ polar moment of inertia of a single crossing area

K slip modulus of crossing areas in N/mm per mm²

m number of longitudinal lamellae within the beam height

n_{CA} number of glue lines between longitudinal and transversal layers within the element thickness

S_y static moment about y-axis

t_{gross} overall thickness of the CLT-element

t_{net} smaller of the sum of the thickness of longitudinal and transversal layers; in CLT-beams usually the sum of the thickness of transversal layers

$t_{net,cross}$ sum of the thickness of transversal layers

$t_{net,long}$ sum of the thickness of longitudinal layers

V transversal force

q_y external load

τ_{eff} shear stress according to the beam theory calculated with the gross cross section

τ_{tor} torsional shear stress acting in crossing areas

$\tau_{xz,gross}$ shear stress calculated with the gross cross section

$\tau_{xz,net}$ shear stress calculated with the net cross section

τ_{yx} unidirectional shear stress parallel to the beam axis acting in crossing areas

τ_{yz} unidirectional shear stress perpendicular to the beam axis acting in crossing areas

6 References

Bejtka, I.: Cross (CLT) and diagonal (DLT) laminated timber as innovative material for beam elements. Karlsruher Berichte zum Ingenieurholzbau, Bd. 17, KIT Scientific Publishing, 2011

Blaß, HJ; Flaig, M.: Stabförmige Bauteile aus Brettsperrholz. Karlsruher Berichte zum Ingenieurholzbau, Bd. 24, KIT Scientific Publishing, 2012

Blaß, H J; Görlacher, R: Zum Trag- und Verformungsverhalten von Brettsperrholzelementen bei Beanspruchung in Plattenebene. In: Bauen mit Holz 104, 2002, H. 11 S. 34-41, H. 12 S. 30-34.

Bogensperger, T; Moosbrugger, T; Silly, G: Verification of CLT-plates under loads in plane. In: Proceedings. 11th World Conference on Timber Engineering, Riva del Garda, Italy, 2010

Bogensperger, T; Moosbrugger, T; Schickhofer, G: New Test Configuration for CLT-Wall Elements under Shear Load. In: Proceedings. CIB-W18 Meeting 40, Bled, Slovenia, 2007, Paper 40-12-3

Bosl, R: Zum Nachweis des Trag- und Verformungsverhaltens von Wandscheiben aus Brettsperrholz. Dissertation, Universität der Bundeswehr, München, Germany, 2002

CUAP 03.04/06: Solid wood slab element to be used as a structural element in buildings. Version June 2005

EN 338, 2009. Structural timber - Strength classes. European Committee for Standardization (CEN), Brussels, Belgium.

EN 1995-1-1, 2004. Eurocode 5. Design of timber structures - Part 1-1: General - Common rules and rules for buildings. European Committee for Standardization (CEN), Brussels, Belgium.

Flaig, M: Biegeträger aus Brettsperrholz bei Beanspruchung in Plattenebene. Dissertation, Karlsruher Berichte zum Ingenieurholzbau, Bd. 26, KIT Scientific Publishing, 2013

Jöbstl, RA; Bogensperger, T; Schickhofer, G: In-Plane Shear Strength of Cross Laminated Timber. In: Proceedings. CIB-W18 Meeting 41, St. Andrews, Canada, 2008, Paper 41-12-3

Jöbstl, RA; Bogensperger, T; Schickhofer, G: Mechanical Behaviour of Two Orthogonally Glued Boards. In: Proceedings. 8th World Conference on Timber Engineering, Lahti, Finland, 2004

Moosbrugger, T; Guggenberger, W; Bogensperger, T: Cross Laminated Timber Wall Segments under homogeneous Shear — with and without Openings. In: Proceedings. 9th World Conference on Timber Engineering, Portland, Oregon, USA, 2006

Schickhofer et al. BSPhandbuch - Holz-Massivbauweise in Brettsperrholz". Technische Universität Graz, holz.bau forschungs gmbh, Karlsruher Institut für Technologie, Technische Universität München, Eidgenössische Technische Hochschule Zürich, 2009

Traetta, G, Bogensperger, Th, Schickhofer, G: Verformungsverhalten von Brettsperrholz-platten unter Schubbeanspruchung in der Ebene. In: 5. Grazer Holzbau-Fachtagung, September 2006

Wallner, G: Versuchstechnische Ermittlung der Verschiebungskenngrößen von orthogonal verklebten Brettlamellen, Diplomarbeit, Institut für Stahlbau, Holzbau und Flächentragwerke, TU Graz, 2004